Biomedical & Pharmacology Journal Vol. **9**(3), 1189-1201 (2016)

Thermal Distribution of Silica Coated Gold Nano Rods in Tissue-like Phantom as *in Vitro* Model for Plasmonic Photo Thermal Therapy

SEYED JAMAL ASHRAFI[1]*, FATEMEH YAZDIAN[1] , ASHRAF SADAT HATAMIAN ZAREMI[1] , JAVAD MOHHAMADNEJAD[1] and RASSOUL DINARVAND [2]

[1]Department of Life Sciences Engineering, Faculty of New Sciences and Technologies, University of Tehran, Tehran, Iran , North Kargar Street, Tehran, Iran.
[2]Nanotechnology Research Centre, Faculty of Pharmacy, Tehran University of Medical Sciences, Tehran.
*Corresponding author E-mail: ashrafi.shmu@gmail.com

http://dx.doi.org/10.13005/bpj/1067

(Received: July 25, 2016; accepted: September 09, 2016)

ABSTRACT

While plasmonic photo thermal therapy (PPTT(as local hyperthermia could act at a high temperature (56°C), It shows more specificity and a shorter time of heating in comparison to traditional (local, regional, and whole body) hyperthermia. But In order to use this advantage, some critical properties of three key parts of PPTT i.e. laser, nanoparticles and tissue condition need optimization. Herein relation between laser power and nanoparticle concentration to induce and stabilize temperatures in phantom is investigated. Gold nanorods as plasmonic nanoparticles were synthesized, purified and coated with silica. SiGNRs characterization shown Nanorods with a length of 40nm, a width of 10.5nm and about 18nm silica coat Plasmon peak was observed at 812nm. Polyacrylamide gels were selected as tissue-equivalent materials. Different concentrations of SiGNR were mixed with polyacrylamide gels. Laser irradiation was done by diode laser 810 nm with power density of 2W/cm2 for 2 min. Laser power density and nano particle concentration were selected as variable parameters. Thermal changes were monitored online and recorded by an infrared camera.The results show that lower concentrations of SiGNR are more suitable for producing uniform thermal distributions in phantoms, while reducing the laser power decreases the heating rate but thermal distribution is not completely uniform. Frequently turning the laser ON/OFF could induce and stabilize suitable temperature ranges.uniform thermal distribution in tumor, heating rate and prepared constant defined temperature for defining time are three qualitative parameters that need optimization during plasmonic photo thermal therapy. Laser, plasmonic nano particles and tissue are three players of PPTT that must optimize so sufficient heat (qualitative and quantitative) prepares against tumor with the least affect toward healthy tissue.

Keywords: Silica coated gold Nanorods, polyacrylamide phantom, NIR laser, hyperthermia, thermal distribution.

INTRODUCTION

Hyperthermia is commonly defined as heating tissue to a temperature in the range of 41–47°C for tens of minutes [1]. Tumors are selectively destroyed in this temperature range because of their reduced heat tolerance compared to normal tissue, which is due to tumors poor blood supply. Hyperthermia causes irreversible cell damage by loosening cell membranes and denaturing proteins. Accumulated evidence has suggested that hyperthermia can induce apoptosis in normal and tumor cells [2, 3]. Normal tissues subjected to hyperthermia are accompanied by some of the normal physiological responses, such as microvascular expansion, rapid breathing, a rapid heartbeat, increased cardiac output, increased blood flow, and increased kidney manufacturing of urine to dissipate heat [4] .But this phenomena will not damage normal tissue. In cancer tissues, the

blood vessels have an irregular architecture[5]. Microvascular permeability and blood circulation differ from those of normal tissues as the temperature increases, they will be damaged seriously [6].

In conventional hyperthermia three methods are common, such as whole-body, regional and local hyperthermia. The aim of local hyperthermia is to increase mainly tumor temperature. Regional hyperthermia could be done by perfusion of a limb, organ or body cavity with heated fluid [8] so the temperature can be elevated to 43°C for duration of 2 h[8]. For whole-body hyperthermia usually the temperature is limited to 42°C and energy losses are minimized[9]. Moderate hyperthermia (41°C<T<46°C) has various effects both at the cellular and tissue levels, In thermoablation, a tumor is subjected to high temperatures of heat >46°C (up to 56°C) causing cells to undergo direct tissue necrosis, coagulation or carbonization.[10]

One can imagine that the use of laser light might revolutionize cancer therapy because of the possibility of controlling and confining the thermal damage to tumors only. The biggest disadvantage of laser therapy is its non-selectivity, however. Both normal and tumor cells in the path of the laser light are damaged. The requirement of high power density is another problem [11]. Most PDT agents become active by a 640 nm laser wavelength, this laser cannot penetrate deep tissue, further, in this area biological molecule could absorb the laser too. An alternative to PDT is photothermal therapy (PTT) in which photothermal agents are employed to achieve the selective heating of the local environment [14,15]. Indocyanine green is one of the PTT agents with maximum absorption at 790 nm which can be located in biological window areas. But the problem with dye molecules is their photo- bleaching under laser irradiation [16] .

During the last decade the development of nanotechnology has provided various nanostructures with exceptional optical properties such as gold nanoshells, gold nanocages, gold nanostars, gold nanorods and gold nanoprisms. It has been reported that these structures enhanced absorption cross section five times bigger than conventional photo absorbing dyes. This property helps producing high temperature with low laser energies. Photostability of nanostructures is another merit of for the use of nanostructurese compared with the photo bleaching weakness of conventional PTT agents. With the attention that heat in this structure comes from plasmonic phenomena, known as plasmonic photothermal therapy (PPTT) agents[17].

By changing the shape of gold nanoparticles to gold nanorods, one can not only change the absorption and scattering wavelengths from visible to the NIR region, but can also increase their absorption and scattering cross sections, NIR tunability [18], ease of surface functionalization for tumor targeting [19], and capability to efficiently convert NIR laser energy to heat [20]. These properties collectively make AuNRs excellent candidates for therapies that selectively destroy cancerous and diseased cells and tissue *in vivo*. The rapid production of heat (56°C) [21] and microbubble formation and cavitation from a thin layer of vaporized fluid surrounding the nano particles are suggested as two mechanisms for tumor ablation by PPTT [22].

The success of PPTT is dependent upon the laser, nanoparticles and cells or tissue interaction. If there is an optimum concentration of nanoparticles and laser parameters for specific tumors, then maximum cell death and minimum side effects will be achieved. Thermal distribution is one of the effective qualitative parameters for thermal therapy that should be optimized. Delivering sufficient and targeted laser to elicit the plasmon particles within deeper and spatially distributed tumor environments is important. For reaching to these purposes and decreasing the effects of healthy tissue on laser absorption/scattering, Bagley and coworkers [40] designed biocompatible, implanted illumination devices that unlike the fiber optics could deliver NIR laser broadly to the large surfaces of deep tumors such as ovarian cancers[40]. GNR as plasmonic nano particle should pass some criteria such as surface modification and having specific size and plasmon peak. Silica layer used for surface modification because it could decrease toxicity and increase photo stability of CTAB coated

GNR, silica layer protects gold nano rods from aggregation in phantom or cell growth media, modification and functionalization of SiGNR is easier than bear GNR. For investigation this correlation between GNR and laser parameter for heat production, we need some things simpler than tissue or tumors. Because using actual tissue may be impractical due to the constraints of accessibility and storage of fresh samples. Reproducibility of results may also be poor because of the difficulty in finding identical specimens or sample preparations[25]. However In order to decrease the complexity of tissue and increase the reproducibility of the result, polyacrylamide gels were selected as the tissue-equivalent phantom. Herein we investigate the correlation of the concentration of silica coated gold nanorods (SiGNR) and laser parameters for preparing sufficient homogenous heat in phantom as a tissue simple model. Gold nanorods were synthesized, purified and coated with a thin layer of silica. Before and after coating they were characterized by TEM and UV/vis spectrophotometry. SiGNRs were dispersed in polyacrylamide gels phantom. Laser irradiations were done for 2 min by 810 nm CW laser. Temperature changes were monitored online by an infrared camera. Data were extracted by IR analytic software, and the results presented as a thermal image (qualitative) and heating rate graph (quantities) data.

MATERIALS AND METHODS

Gold (III) chloride trihydrate (HAuCl4, >99%; Sigma), sodium borohydride (NaBH4, Sigma-Aldrich), cetyltrimethylammonium bromide (CTAB, sigma), ascorbic acid (sigma, 99%), silver nitrate (AgNO3, >99% Aldrich*),* Acrylamide (sigma 99%,), *N, N* –dimethylenebisacrylamide (98%), ammonium persulfate (APS 98%, sigma), Sodium chloride (sigma-AIdrich), and *N, N, N, N* – tetramethylenediamine (TEMED 99%, sigma-Aldrich) were used as purchased. Tetraethyl ortho-silicate (TEOS) and methanol prepared from Merck (Germany), ultrapure deionized water (Zolalan Co., Tehran, IR) were used for all solution preparations and experiments.

Gold nanorod synthesis: AuNRs were synthesized following a modified procedure described previously [23]. In short, the seed solution was prepared using 0.25 ml of an aqueous 0.01 M solution of HAuCl4 · 3H2O, 7.5 ml of a 0.10 M CTAB solution in a beaker. Following that, 0.6 ml of an aqueous 0.01 M ice cold NaBH4 solution was added which made the solution turn into a bright brown color, actually it indicates formation of Au seed. Subsequently, Seed the solution was aged for 2.5 hours at 25–28°C. Growth solution was prepared by the addition of 9.5 ml of 0.1 M CTAB, 0.4 ml of 0.01 M HAuCl4 · 3H2O, and 0.03 ml of 0.01 M AgNO3 in respective order one by one to achieve a bright orange/yellow color. To that, 0.064 ml of 0.1 M ascorbic acid was added which immediately turned the solution colorless. Finally, 0.010 ml of the seed solution was added, gently mixed and left undisturbed for at least 20 h at 28°C.

Silica coating of gold nanorods (SiGNR): Mesoporous silica coating on AuNRs was carried out according to the Gorelikov and Matsuura protocol with some modifications[24].The synthesized AuNRs were washed by centrifugation (40 mL aliquots at a time, at 9500 rpm for 25 min). The residue was diluted to 20 mL by adding water. Then, 200 µL of 0.1 M NaOH solution was added upon stirring. Following this step, three 60µL injections of 20% TEOS in methanol were added under gentle stirring at 30 minute intervals. The mixes were reacted for 3 days at 26~28°C.

Preparation of polyacrylamide phantoms containing SiGNRs : Polyacrylamide phantoms were prepared as described by Jang et al[35] . An acrylamide stock solution was prepared by mixing acrylamide (1.3 g), *N*, *N*–methylene bisacrylamide (1 mg), and sodium chloride (52 mg) in distilled water (3.635 mL). The acrylamide stock solution (233 µL), an aqueous solution containing SiGNRs (260 µL), a 10% aqueous APS solution (3 µL), and TEMED (2 µL) was added to a plastic tube in serial order and mixed by a vortex. These phantoms were allowed to gelation for 2 hours. For the next day's experiments they were stored at 4°C to prevent water evaporation and nano particle doping in phantom. In each experimental batch, the final particle concentrations of GNRs in the

prepared phantoms were 6.25, 12.5, 25, 50, and100 µg/mL.

Laser treatment and temperature monitoring in phantoms: The phantom which was in a 2-ml plastic microtube containing 1 ml of SiGNR gel was transferred to room temperature. Laser illumination was done by an 810 nm laser (DenLase-810/7, Beijing, China) laser probe (spot size 4 mm) fixed at the top of the microtube with a 12-mm distance from the surface of the gel. Two types of experiments were done: one type included a fixed laser power density (2W/cm^{-2}) and a different concentration of SiGNR, and the second type with a fixed concentration and a different laser power density (2000 mW, 750 mW, 350 mV and 250 mW). At same time temperature changes in the SiGNR phantom were monitored and recorded by infrared camera (ITI P-240, Stockholm, Sweden). Temperature changes were analyzed from the surface of the gel to a 9-mm depth. For each phantom, maximum, average, and minimum temperatures were recorded during laser illumination automatically by IR software. Temperature data were extracted from the recorded images and video by IR camera and its software (ITI IrAnalyzer ver 2011). Temperature changes (ΔT) of phantoms at each point P *i* (i =maximum, average and minimum) after irradiation time *t* was calculated using the equation (1):

$$\Delta T(x_i, t) = T(x_i, t) - T(x_i, 0)$$

Where *x i* is the depth of point P *i* and *T* (x i, *t)* is the measured temperature of P *i* at time *t.*

UV/Vis Measurement. Absorbance spectra were acquired by ultraviolet to visible (UV/Vis) extinction spectroscopy (Teifsanj pishro pajohesh Co, IRAN). For this purpose 2 ml of GNR or SiGNR that after centrifugation dispersed in deionize water transfer to quartz cell with 1cm wavelength path. Before the measurement machine blanked with 2 ml deionize water. Absorbance spectra collected from 450 nm to 1100 nm with 1 nm steps at room temperature.

TEM imaging

For TEM imaging 2ml of 2 times washed of GNR or SiGNR dispersed in deionized water and sonicated (Ultrasonic development and technology Co, IRAN) for 5 min, after it 100micro liter of this suspension dropped on the 300mesh carbon coated copper grid (ISP, USA) and allowed to dry for 15 min at room temperature. This grid imaged by 80 KV TEM (EM10C, Zeiss, Germany).

RESULT AND DISCUSSION

UV/Vis spectrophotometry of CTAB coated gold nanorods displayed two plasmonic peaks (transverse and longitudinal) at 510nm and 806 nm (Figure 1a) corresponding to the anisotropic structure of gold nanorods. TEM micrograph confirmed synthesis of the GNR with an aspect ratio 3.8 with 10±1.3 nm width and 40±2.1 nm lengths (Figure 1b). Jaque et al[45]

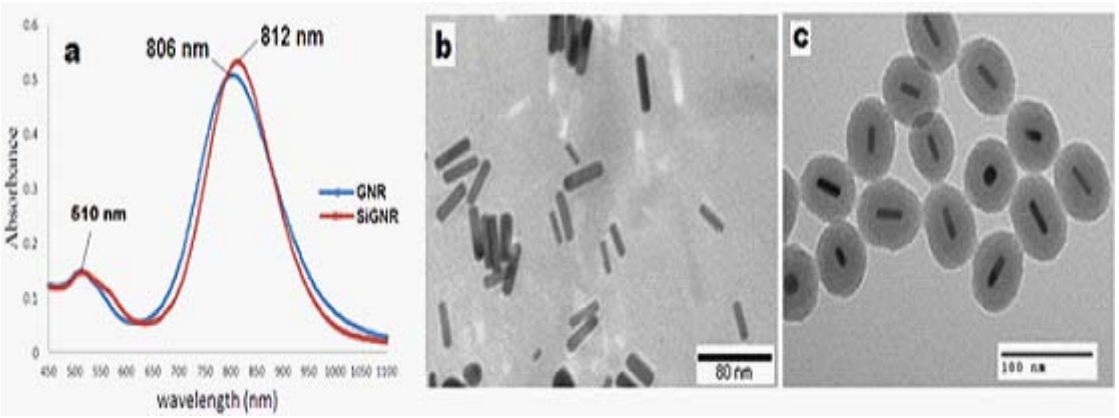

Fig 1: TEM micrograph of synthesized gold nano-rods a) silica coated gold nano-rods b) UV/Vis spectrum of GNR (806 nm) and SiGNR.(812 nm).

discussed that why gold nano rods better than other plasmonic nano particle such as gold nano shell, gold nano stars , and gold nano particles briefly because maximum laser absorption (minimum scattering) observe in these structures. We tried for synthesis GNR with aspect ratio 3.5-3.8 because this size reported as the most effective GNR for PPTT[51]. CTAB coated GNR shows different disadvantages for in vivo and in vitro experiments. For example, they are very toxic and sensitive to chemical and biological components so that usually these nano-particles in bare form will aggregate and precipitate [26]. High intensity or long time laser irradiation could melt and change the morphology of GNR over certain energy thresholds [31]. Different techniques such as polyelectrolyte coating (poly (4-styrenesulfonic acid) PSS,…), ligand exchange (SH-PEG) coating (phospholipid, silica, …) [27-30] have been developed by researchers to overcome the drawbacks of CTAB-GNR.

Replacing the CTAB coating layer with silica not only allows heat dissipation from the surface of GNR quickly, but also will increase photo thermal stability of GNRs[32].UV/Vis spectrophotometry shown second peak of GNR shift from 806nm to 812 nm for SiGNR while first plasmon peak remained fixed at 510 nm for both of them (Figure 1a). This phenomenon could be explained by the fact that the local refractive index of the silica shell (1.45) was larger than water (1.33). [33] TEM micrograph clearly showed a silica layer about 18 ±2 nm in thickness uniformly coating the surface of gold nanorods (Figure 1c).

Not only CTAB GNR is toxic and inapplicable for *in vivo* hyperthermia, but also it is sensitive to phantom component so when it's mixed by polyacrylamide gels, aggregation and precipitation observed in bottom of phantom (Figure S3, b), while silica layer protected GNR from aggregation and successfully dispersed it in phantom (Figure S3, c).

Polyacrylamide gels were selected as the base phantom because they are transparent, solid, homogeneous, reproducible, and their optical–thermal properties will not change with temperature. Laser irradiation was done by laser fiber with 4mm spot size and 12mm, distance from top of the gels in Microtube (Figure 2a, b), IR camera (Figure 2d) monitors temperature changing in phantom online and sent data to IR analyzer software (Figure 2e). White-light image (Figure 2f , Figure s3 C) of Individual phantom clearly shows that SiGNR mixed homogeneously with the polyacrylamide gels and this colors and phantom morphology were stable when phantom temperature reached to 70°C during laser

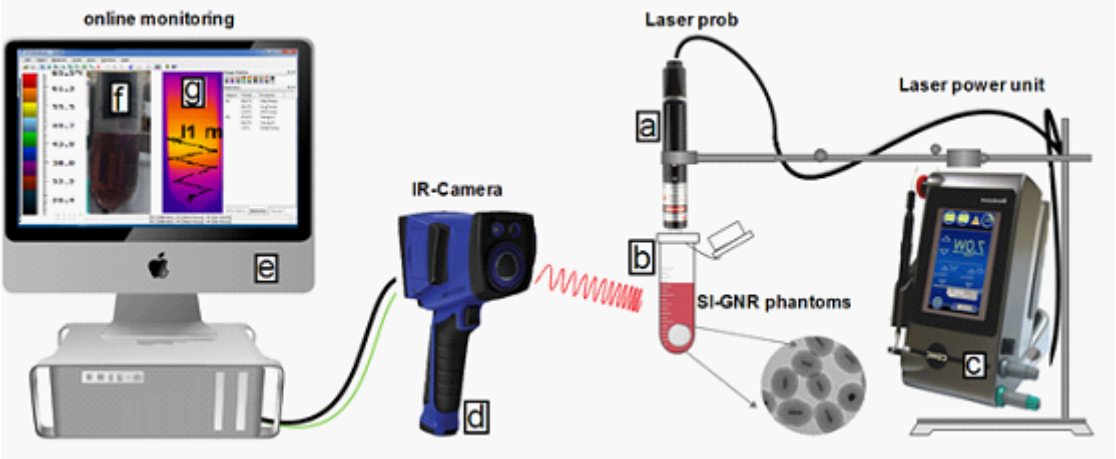

Fig 2 : Setup of thermal measurement experiment: laser probe a), microtube contains different concentrations of SiGNR b), laser machine c), infrared camera d), IR analyzer software e), polyacrylamide phantom contains 100 µg/ml SiGNR f), thermograph of SiGNR phantom and ragged line from surface to bottom of gels includes maximum, minimum and average points of temperature.

irradiation. As shown in thermal image (Figure 2g), ragged line from the surface of the gels (middle part of microtube) to bottom of gels completely covers the SiGNR gels horizontally and vertically. On the ragged line during the laser illumination three points, such as maximum, average and minimum, were determined automatically by the IR camera software. Indeed Location of this point was not fixed in depth of gels so dependent to temperature change its location will change on the ragged line. For homogenous thermal distribution these three points are very near to each other, even sometimes are overlaps. We used ragged line because it could cover all the phantom area, in plus without this ragged line IR camera automatically will select a minimum temperature point out of the phantom usually tube rack that used for fixing microtube during the experiments

In Figure 3 thermal images of different concentrations of SiGNR gels show that constantly maximum temperatures were observed at the surface or at 1-2 mm depth of the gels, at the contact point of the laser spot and gels. But at the low concentration of SiGNR thermal distribution is more uniform, interestingly maximum temperature point observed at the bottom of the phantom (Figure 3, 6.25µg/ml) No SiGNR aggregation or precipitation observed in phantoms. One reason is that in low concentrations of SiGNR the laser could pass through the phantom, but in high concentrations the depth of laser penetration is low (Figure S1). For high concentration SiGNR Not only laser beam penetration is low and thermal distribution is not uniform, but also the temperature of the empty area at the top of the gel surface (middle to up part of microtube) increased rapidly during the laser illumination. This temperature increase could change from 25 - 8°C at distance 2-8 mm above the surface of the gel (Figure S2).

Quick temperature changes at the surface of the high concentration SiGNR gels could transfer to the top atmosphere of the gels or evaporate the water content of the gels at the surface. An et al [34] observed this heat convention at the surface of the GNR solution during irradiation by 1W/cm2 , 808 nm laser. But for low concentrations of SiGNR that temperature alteration is more uniform and slower; only the bottom half of the phantom gels displayed temperature changes. These results are similar to the work of Jang et al [35]. The numerical investigation by Tan and Yu [36] indicated the radiative transfer in the semitransparent media is the crucial factor which leads to such a peculiar temperature distribution.

Quantitative analysis of temperature changes confirmed that at high concentrations of SiGNR gels the temperature will increase very quickly on the surface of the gels, and the thermal distribution in the phantom is not uniform and homogeneous (Figure 4). Thermal changes from laser irradiation (2min, laser 810 nm, 2W) were shown as gradient of ΔT during the time. For each concentration of SiGNR (a= 100µg/ml, b=50µg/ml, c=25µg/ml, d=12.5µg/ml, e=6.25µg/ml, f=0µg/ml) a separate graph show ΔT gradient change along the phantom. For each graph three curves related to minimum, average and maximum temperature presented. Heating Rate of each point and concentration present useful data. Remarkably, the location of each curve (min, avr, max) presents the qualitative data that extracted from thermal images. In other word when thermal distribution is uniform curve rate and the location of three points are very

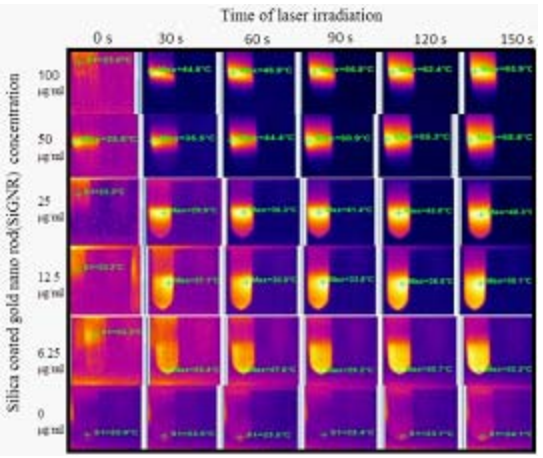

Fig 3: Thermal images of suspended phantom including different concentrations (6.25, 12.5, 25, 50, 100 µg/ml) of SiGNR irradiated by 810 nm, 2W/cm^{-2} for 150 s. Low concentrations show uniform thermal distribution only in gels, but for high concentrations it is not uniform, and there is some temperature transfer to the air at the top of the gel surface.

near or overlapped. It is clear that at high concentrations (Figure 4 a,b) of SiGNR phantom not only quickly temperature increase at the maximum point (usually the surface of the phantom), but also this temperature distribution is so slow that the average point and the minimum point are far from the maximum point. As mentioned these three point select automatically by IR analysis software on ragged line in phantom according to temperature changes during laser irradiation. It shows that all of the laser energy absorbed and changed to heat at the surface of the phantom (Figure 3). From this results two note could be understood, first, high concentration of SiGNR in phantom limited laser beam penetration (like figure S1) however, all the laser energy converts to heat at the surface of phantom ,at the place of laser and phantom contacts. Second, the source of heat at bottom layer is convection phenomena from plasmonic heated top layer (like figure S2). How ever could say that thermal distribution for unsuitable concentration of plasmonic nanoparticles is not uniform along the 9 mm polyacrylamide gels as tissue-equivalent materials.

By decreasing the concentration of SiGNR in the phantom, the heating rate and ΔT gradient will decrease to a minimum level, and the thermal difference between three points (max, aver and min) of the phantom will drop so that uniform thermal distribution in the phantom is observable (Figure 4, d and e). In the interim, this phantom is a very simple model of tissue, actually it is static and cannot change the produced heat, while in tissue or tumor blood flow could affect heating rate during the time. However , most important note from this experiment is a correlation between the laser and the SiGNR concentration of preparing uniform thermal distribution.

The effects of laser power density of the thermal distribution and heating rate were investigated by the use of different laser powers (Figure 5a-d). The concentration of SiGNR phantoms was fixed at 100µg/ml. The laser power density was adjusted to a= 2W/cm2, b= 0.7 W/cm2, c= 0.35 W/cm2 and d= 0.25 W/cm2. As is shown in Figure 5 decreasing the laser power density could change the temperature rate, but thermal distribution was not uniform along the phantom. The inset thermal image of each graph confirms the maximum temperature observed at the contact point of the laser beam and the gel surfaces. These results confirm the previous experiments with

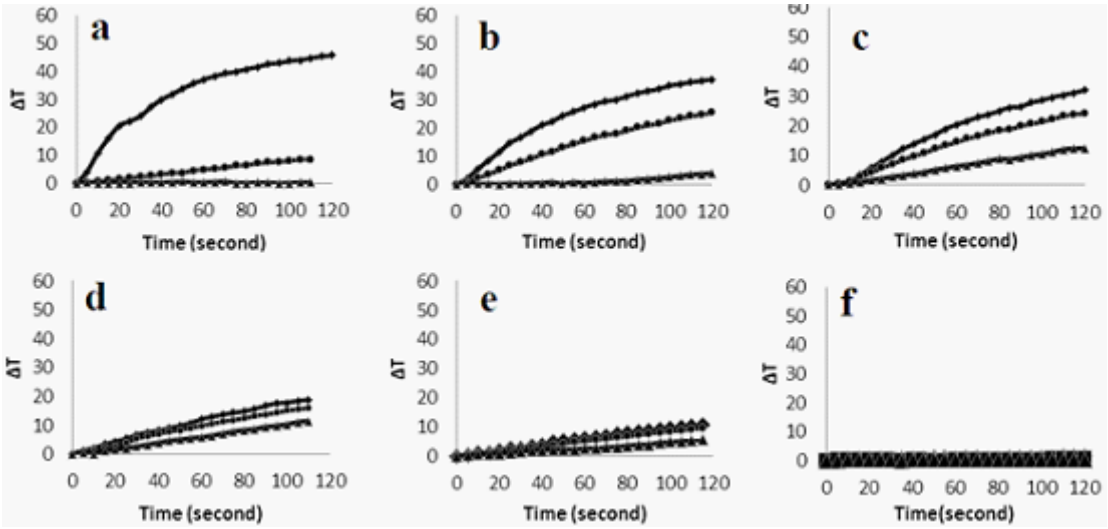

Fig 4: Quantitative analysis of thermal distribution in phantom (a= 100µg/ml, b=50µg/ml, c=25µg/ml, d=12.5µg/ml, e=6.25µg/ml, f=0µg/ml) irradiated by 810 nm, 2W/cm^{-2} for 120 s. Each plot shows maximum (■, average (•), minimum (▲) temperature in 9 mm phantom, as it shows decreasing the concentration made more uniform thermal distribution so the minimum and maximum temperature points are not far from each other, while the temperature change rate got slower.

different concentrations of SiGNR and fixed laser power density (Figures 2 and 3). In both experiments improper concentration of SiGNR cannot prepare applicable thermal distribution pattern in phantom.

Jang et al, [35] investigated the effect of PEG-GNR concentrations for thermal distribution in polyacrylamide gels with different concentrations of PEG-GNR from 0.5 nm to 5 nmol irradiated by 2W/cm2 and 5W/cm2 laser power density. The Results of this research were similar to Jang et al that reported, in order to reach uniform thermal distribution, concentration of GNR is more important than the laser power density actually they suggested the lowest (0.5 nmol) concentration of GNR could prepare uniform thermal distribution in phantom. We believe that two remark about their works should be attention. One, if SH-PEG coat could increase the chemical stability of GNR, but this layer could not prepare enough photo thermal stability especially for a long time or high power laser illumination[45]. Two, when reaching a therapeutic temperature (41-46°C) for at least 30 minutes is needed. Heating rate cannot be too slow; because blood flow in the tumor tissue could cause the heat to dissipate if a slow heating rate is employed, especially for tumors located in regions with high blood flow such as the liver, kidneys and lungs. Other side the therapeutic effect of hyperthermia depends on temperature and exposure time. Actually, this correlation discussed in detail from basic to professional level[47-50]. At temperatures above 42.5-43°C the exposure time can be halved for each 1°C temperature increase and still give an equivalent cell kill [37]. While most normal tissue could tolerate for 1 h up to 44°C[38], it is reported that 42-42.5°C could permanently damage the central nervous system if applied for longer than 40-60 min [39].

Plasmonic photothermal therapy (PPTT) as local hyperthermia or thermal ablation at very high temperatures could destroy the cancer cells in tumors by coagulating the proteins in them and collapsing nearby blood vessels. For example, Shen et al [41]. Ablating the tumor cells in mouse models by silica coated GNR and 3W/cm2 NIR laser so that after 30 seconds the temperature changed from 31.5°C to 65.9°C. Reaching a therapeutic temperature (42-43°C) from body temperature (37°C), needing ΔT=5-6°C, is possible even at the lowest concentration of SiGNR (Figure 4, e) or laser power density (Figure 5). But inducing

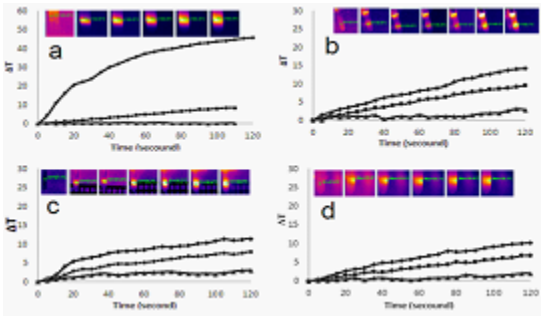

Fig 5: Plot of thermal distribution for 100µg/ml SiGNR phantom, irradiated by810 nm with different power densities (a=2000 mW/cm^{-2}, b=750 mW/cm^{-2}, c=350 mW/cm^{-2}, d=250 mW/cm^{-2}). Each plot shows maximum (■), average (●), minimum (▲) temperature in 9 mm phantom. It shows that decreasing laser power density could not make uniform thermal distribution in phantoms; thermal image insets in each plot confirm thermal is not homogeneous in phantoms.

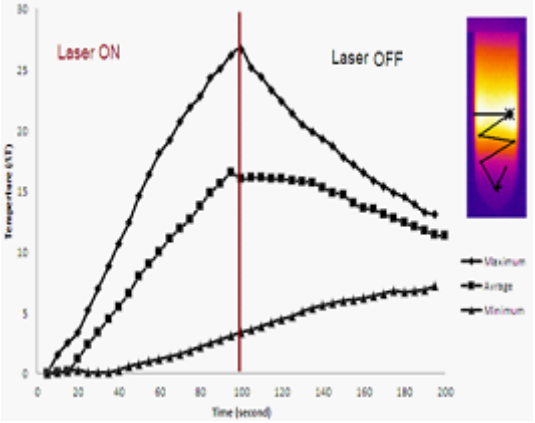

Fig 6: Temperature changes during laser illumination 810 nm, 2W/cm^{-2}, of SiGNR (50µg/ml) phantom. Left side of red line shows the temperature increasing rate when the laser is ON. Right side shows heat rate dissipation when the laser is OFF. For the minimum temperature point heat dissipation does not happen because this heat comes from distributed temperature at the top, not from laser illumination.

and preserving this temperature for a long time is challenging too. Thermo ablation need ΔT=18-23°C For about 5 minute[46]. Although necessary time is shorter, but the question is that how we can induce and stabilize this temperature? While the heating rate shown, every 1 minute about 6-30°C temperature will increase in phantom (figure 4). For solving this problem we suggest that by turning the laser on and off frequently, it is possible to manage temperature increasing and decreasing for stay at wanted temperature range. Again, apply of unsuitable concentration of SiGNR cannot be logic for stabilizing the wanted temperature for a specific time. At high concentration of SiGNR phantom we observed a high rate of increasing temperature (laser on) and a high rate of heat dissipation (laser off) will happen. Actually ramp of temperature increase and decrease approximately happened with the same rate. (Figure 6) Interestingly, for the minimum temperature point, after the laser was off, not only did cooling not happen, but also the temperature increased, which shows the source of the temperature is not direct laser power or PPTT. This temperature comes from the top layer that is produced during PPTT phenomena. We should keep in mind that this occurrence for marginally healthy tissue during *in vivo* experiments would not be a pleasure and should be of concern. It is expected that *in vivo* experiments on tumors with leaky vasculatures and blood flow effect of heat dissipation, temperature management will be more challenging.

Another technical challenge for determination of the correct dosage of hyperthermia is the lack of a noninvasive system for monitoring the temperature for *in vivo* studies. Modeling, design of thermal sensitive materials, computer simulation and tissue-equivalent phantoms have been suggested as multi-pronged approaches to solve this problem[10,52]. With this problem in mind, we selected polyacrylamide phantoms for estimating and modeling the effective duration of laser illumination for specific laser power densities and SiGNR concentrations. Recently an infrared thermal camera has successfully and precisely monitored and presented thermal changes in subcutaneous tumors and marginally healthy tissues during hyperthermia [10]. We believe that temperature monitoring of tumor is more important and essential for successful PPTT at in vivo experiments, because the frequency of laser on and off for inducing and holding appropriate temperature in tumor dependent to the feedback of a temperature monitoring system.

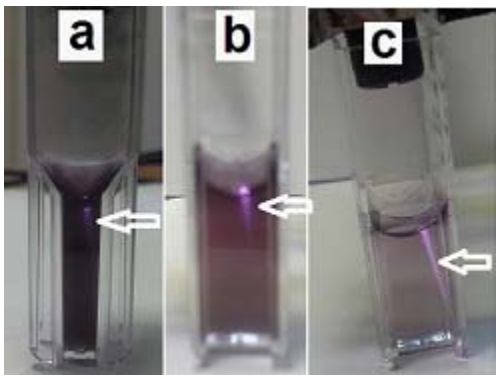

Fig S1: Laser beam is observable as purple shine in each phantom. Decreasing the concentration of SiGNR produces more laser penetration in the phantom As a result thermal distribution is more uniform in a low concentration of nanoparticles.

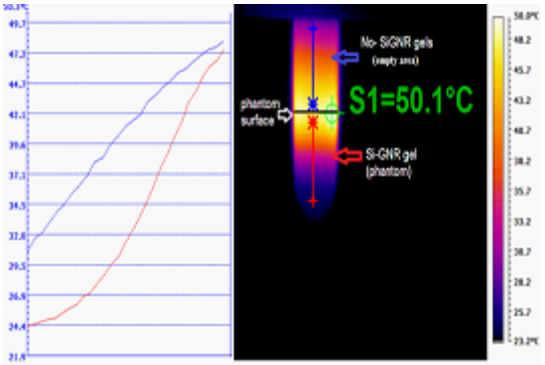

Fig S2: Laser illumination (2W/Cm^{-2}, 810 nm, 2 min) of SiGNR (50µg/ml) phantom, showing bottom half of microtube that contains suspended SiGNR in polyacrylamide gels. During laser illumination, the temperature changed from 24.4°C(minimum) to 49.7°C (maximum) (red line) in PPTT phenomena. Interestingly, the top half of the phantom which is empty (no SiGNR gels) shows a change from 31°C (minimum) to 50°C (maximum) and that this heat comes from convention at the surface of SiGNR phantom after laser illumination

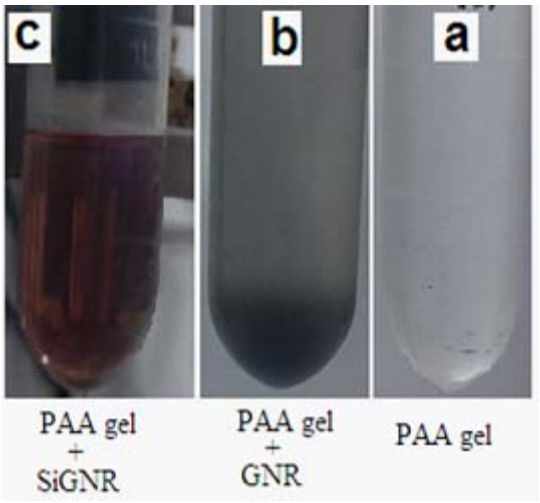

Fig s3: while- light image of polyacrylamide gels (PAA) a) aggregation and precipitation of CTAB coated nano rods after mixing with this gels b) uniform distribution of mixed Silica coated GNR with PAA gel c)

Providing moderate temperature (41-47°C, >60 min) for traditional hyperthermia suffers from some challenges such as unavoidable heating of healthy tissue, limited penetration of heat into body tissues by microwave, laser and ultrasound energy, and thermal under-dosage in the target region. [44] While PPTT as local hyperthermia could solve some of these challenges because it is a more targeted method, the temperature could increase to 56°C, which for 4-6 min is enough for tumor ablation[46]. Actually, it appears that the dose-response curves for hyperthermia look similar to those for radiation or drug dosages. However, the challenge is to understand the critical cellular targets of thermal inactivation, both in cancer cells as well as in the surrounding healthy cells. [42, 43]

PPTT hyperthermia requires attention to the interaction of the laser, nanoparticles and biological aspect. For each of these, many effective parameters exist that must be optimized in order to achieve a feasible protocol for the application of PPTT for clinical purposes.

These parameters are various and include the following; laser wavelength, laser power density, laser type (CW or pulse), type of laser application (external or internal irradiation), and laser program for inducing and stabilizing heat for wanting duration. They also include many factors regarding nanoparticles, such as the type of plasmonic nanoparticles, their shape, size, optical properties (absorbance, scattering), surface coating, biostability, photo stability, biocompatibility, concentration, purity and degree of specification to cells or tumors. In addition, regarding biological criteria, there are parameters for the type of cells or tissue, their size, location, blood flow, type and location of healthy tissue, tissue optical properties and laser interaction.

For reaching to clinical application of PPTT not only mentioned parameter should be attention, but also strategies or plan is needed. For example, Issels et al[48] have introduced six biological and clinical capabilities defined as 'hallmarks of hyperthermia' to emphasize the pleiotropic effect induced by heat in malignant cells and tissues. They suggest that hallmark could help researchers for reginal hyperthermia as targeted thermal therapy, however, we believe that PPTT could consider this clinical plan too, even it is apply more effective by targeting the laser and plasmonic nano particles. Indeed, this is typically achieved by decorating of nanoparticles with peptides and antibodies that allow tumor-specific homing and accumulation[49]. Simulation and modeling could be useful for design clinical plan for hyperthermia treatments of tumors[53]. Investigation efficacy of obtaining results of this research in more complicated phantom that like tissue could dynamically react to plasmionic heat is next our goals.

CONCLUSION

Recent advances in our understanding of fundamental properties of nanoparticles provide a framework for the use of nanoparticles as conduits for generating hyperthermia. Plasmonic photo thermal therapy that used as an anisotropic gold nano structure for targeting the laser toward the tumors has recently gotten high promise. Herein we synthesis GNR that could absorb laser wave length in biological windows (812nm). Surface modification of GNR has done by a silica layer (SiGNR). polyacrylamide gel phantoms were selected as tissue-equivalent materials, SiGNRs were dispersed in different concentrations in this phantom and laser illumination performed utilizing

a diode laser 810 nm, 2W/cm2 for 2 min. Correlation between SiGNR concentration and laser parameter for preparing uniform thermal distribution in phantom presented as qualitative and quantitative data. Frequently turning, laser on/off suggested as a method for inducing and preserving wanted temperature in tissue. While necessary to have a noninvasive and precise method for monitoring the temperature in tissue exist. Possibility of thermal transfer to healthy margin tissue from the improper concentration of plasmonic nano particles shown and confirmed the importance of this parameter for hyperthermia. While this result is logic, but for transferring theme to clinical application it should repeat in phantom or condition that are more similar to *in vivo* condition like tissue or tumor.

ACKNOWLEDGMENT

Financial support from the Iranian Nanotechnology Initiative Council is gratefully acknowledged. Special thanks to Dr. Nasim Chiniforoush for her support during use of laser equipment and Connie Allison for manuscript editing.

REFERENCES

1. Svaasand LO, Gomer CJ, Morinelli E. On the physical rationale of laser induced hyperthermia. *Lasers in Medical Science.***5**(2):121-128.
2. Tronov V, Konstantinov E, Kramarenko I. [Hyperthermia induced signal for apoptosis and pathways of its transduction in the cell]. *Tsitologiia.* **44**(11):1079-1088 (2001).
3. Brade AM, Szmitko P, Ngo D, Liu F-F, Klamut HJ. Heat-directed suicide gene therapy for breast cancer. *Cancer gene therapy.* **10**(4):294-301 (2003).
4. Horsman MR. Tissue physiology and the response to heat. *International journal of hyperthermia.* 22(3):197-203 (2006).
5. Nikfarjam M, Muralidharan V, Malcontenti Wilson C, Christophi C. Progressive microvascular injury in liver and colorectal liver metastases following laser induced focal hyperthermia therapy. *Lasers in surgery and medicine.* **37**(1):64-73 (2005).
6. Eddy HA, Chmielewskig G. Effect of hyperthermia, radiation and adriamycin combinations on tumor vascular function. *International Journal of Radiation Oncology* Biology* Physics.* **8**(7):1167-1175(1982).
7. Myerson R, Moros E. Roti Roti JL. Hyperthermia. *Principles and Practice of Radiation Oncology, 3rd edition. Philadelphia: Lippincott-Raben Publishers*.637-683 (1997).
8. Coit DG. Hyperthermic Isolation Limb Perfusion for Malignant Melanoma: A Review: Concise Reviews In Surgery. *Cancer investigation.* **10**(4):277-284 (1992).
9. Robins H. Systemic Hyperthermia Oncological Working Group. *Oncology.* **52**(3):260-263 (1995).
10. Kumar CS, Mohammad F. Magnetic nanomaterials for hyperthermia-based therapy and controlled drug delivery. *Advanced drug delivery reviews.* **63**(9):789-808 (2011).
11. Pissuwan D, Valenzuela SM, Killingsworth MC, Xu X, Cortie MB. Targeted destruction of murine macrophage cells with bioconjugated gold nanorods. *Journal of Nanoparticle Research.* **9** (6):1109-1124 (2007).
12. Wilson B, Patterson M. The physics of photodynamic therapy. *Physics in medicine and biology.* **31**(4):327 (1986).
13. Gold MH. Introduction to photodynamic therapy: early experience. *Dermatologic clinics.* **25** (1):1-4 (2007).
14. Anderson RR, Parrish JA. Selective photothermolysis: precise microsurgery by selective absorption of pulsed radiation. *Science.***220**(4596):524-527(1983).
15. Camerin M, Rello S, Villanueva A, et al. Photothermal sensitisation as a novel therapeutic approach for tumours: studies at the cellular and animal level. *European Journal of Cancer.* **41**(8):1203-1212 (2005).
16. Chen WR, Adams RL, Heaton S, Dickey DT, Bartels KE, Nordquist RE. Chromophore-enhanced laser-tumor tissue photothermal interaction using an 808-nm diode laser.

Cancer Letters. (1):15-19 (1995).
17. Huang X, Jain PK, El-Sayed IH, El-Sayed MA. Plasmonic photothermal therapy (PPTT) using gold nanoparticles. *Lasers in medical science.* **23**(3):217-228 (2008).
18. Zhang G, Jasinski JB, Howell JL, Patel D, Stephens DP, Gobin AM. Tunability and stability of gold nanoparticles obtained from chloroauric Acid and sodium thiosulfate reaction. *Nanoscale research letters.* **7**(1):337 (2012).
19. Goldberg SN. Radiofrequency tumor ablation: principles and techniques. *European Journal of Ultrasound.* **13**(2):129-147 (2001).
20. Brunetaud J, Mordon S, Maunoury V, Beacco C. Non-PDT uses of lasers in oncology. *Lasers in medical science.* **10**(1):3-8 (1995).
21. Steger A, Lees W, Walmsley K, Bown S. Interstitial laser hyperthermia: a new approach to local destruction of tumours. *Bmj.* **299**(6695):362-365 (1989).
22. Masters A, Bown S. Interstitial laser hyperthermia in tumour therapy. Paper presented at: Annales chirurgiae et gynaecologiae.(1989).
23. Sau TK, Murphy CJ. Seeded high yield synthesis of short Au nanorods in aqueous solution. *Langmuir.* **20**(15):6414-6420 (2004).
24. Gorelikov I, Matsuura N. Single-step coating of mesoporous silica on cetyltrimethyl ammonium bromide-capped nanoparticles. *Nano letters.* **8**(1):369-373 (2008).
25. Iizuka MN, Sherar MD, Vitkin IA. Optical phantom materials for near infrared laser photocoagulation studies. *Lasers in surgery and medicine.* **25**(2):159-169(1999).
26. Zhang Z, Wang L, Wang J, et al. Mesoporous Silica Coated Gold Nanorods as a Light Mediated Multifunctional Theranostic Platform for Cancer Treatment. *Advance Materials.* **24**(11)(2012).
27. Hauck TS, Ghazani AA, Chan WC. Assessing the effect of surface chemistry on gold nanorod uptake, toxicity, and gene expression in mammalian cells. *Small.* **4**(1):153-159 (2008).
28. Niidome Y, Honda K, Higashimoto K, et al. Surface modification of gold nanorods with synthetic cationic lipids. *Chem. Commun.* (36):3777-3779 (2007).
29. Fernández-López C, Mateo-Mateo C, Alvarez-Puebla RA, Pérez-Juste J, Pastoriza-Santos I, Liz-Marzán LM. Highly Controlled Silica Coating of PEG-Capped Metal Nanoparticles and Preparation of SERS-Encoded Particles†. *Langmuir.* **25**(24):13894-13899 (2009).
30. Leonov AP, Zheng J, Clogston JD, Stern ST, Patri AK, Wei A. Detoxification of gold nanorods by treatment with polystyrenesulfonate. *Acs Nano.* **2**(12):2481-2488 (2008).
31. Link S, Burda C, Mohamed M, Nikoobakht B, El-Sayed MA. Laser photothermal melting and fragmentation of gold nanorods: energy and laser pulse-width dependence. *The Journal of Physical Chemistry A.* **103**(9):1165-117 (1999).
32. Chen Y-S, Frey W, Kim S, et al. Enhanced thermal stability of silica-coated gold nanorods for photoacoustic imaging and image-guided therapy. *Optics express.***18**(9):8867-8878 (2010).
33. Liz-Marzán LM, Giersig M, Mulvaney P. Synthesis of nanosized gold-silica core-shell particles. *Langmuir.***12**(18):4329-4335 (1996).
34. An W, Zhu Q, Zhu T, Gao N. Radiative properties of gold nanorod solutions and its temperature distribution under laser irradiation: Experimental investigation. *Experimental Thermal and Fluid Science.* **44**:409-418 (2013).
35. Jang B, Kim YS, Choi Y. Effects of Gold Nanorod Concentration on the Depth Related Temperature Increase During Hyperthermic Ablation. *Small.* **7**(2):265-270 (2011).
36. Tan H, Yu Q. 'Numerical Analysis of Temperature Field in Materials During Infrared Heating. *Chinese J. Infrared and Millimeter Waves.* **10**:169-178 (1991).
37. Raaphorst G. *Fundamental aspects of hyperthermic biology.* **10:**(1990).
38. LG LFF. Pathological effects of hyperthermia in normal tissues. *Cancer Research.* **44**(10 Supplement):4826s-4835s (1984).
39. Sminia P, Zee JVD, Wondergem J, Haveman

J. Effect of hyperthermia on the central nervous system: a review. *International journal of hyperthermia.* **10**(1):1-30 (1994).

40. Bagley AF, Hill S, Rogers GS, Bhatia SN. Plasmonic photothermal heating of intraperitoneal tumors through the use of an implanted near-infrared source. *ACS nano.* **7**(9):8089-8097 (2013).
41. Shen S, Tang H, Zhang X, et al. Targeting mesoporous silica-encapsulated gold nanorods for chemo-photothermal therapy with near-infrared radiation. *Biomaterials.* **34**(12):3150-3158 (2013).
42. Jordan A, Scholz R, Schüler J, Wust P, Felix R. Arrhenius analysis of the thermal response of human colonic adenocarcinoma cells in vitro using the multi-target, single-hit and the linear-quadratic model. *International journal of hyperthermia.* **13**(1):83-88 (1997).
43. Frazier N, Ghandehari H. Hyperthermia approaches for enhanced delivery of nanomedicines to solid tumors. *Biotechnology and bioengineering.* **112**(10):1967-1983 (2015).
44. Tanaka K, Ito A, Kobayashi T, et al. Heat immunotherapy using magnetic nanoparticles and dendritic cells for T-lymphoma. *Journal of bioscience and bioengineering.* **100**(1):112-115 (2005).
45. Hu, Xiaoge, and Xiaohu Gao. "Multilayer Coating of Gold Nanorods for Combined Stability and Biocompatibility." *Physical chemistry chemical physics/ : PCCP* 13.21 : 10028–10035 (2011).
46. Jaque D, Maestro LM, Del Rosal B, Haro-Gonzalez P, Benayas A, Plaza JL, Rodriguez EM, Sole JG. Nanoparticles for photothermal therapies. Nanoscale. **6**(16):9494-530 (2014).
47. Dewhirst MW, Viglianti BL, Lora-Michiels M, Hanson M, Hoopes PJ. Basic principles of thermal dosimetry and thermal thresholds for tissue damage from hyperthermia. International Journal of Hyperthermia. 1;**19**(3):267-94 (2003).
48. Issels R, Kampmann E, Kanaar R, Lindner LH. Hallmarks of hyperthermia in driving the future of clinical hyperthermia as targeted therapy: translation into clinical application. International Journal of Hyperthermia. 2;**32**(1):89-95 (2016).
49. Kaur P, Aliru ML, Chadha AS, Asea A, Krishnan S. Hyperthermia using nanoparticles–Promises and pitfalls. International Journal of Hyperthermia. 2;**32**(1):76-88 (2016).
50. Yarmolenko PS, Moon EJ, Landon C, Manzoor A, Hochman DW, Viglianti BL, Dewhirst MW. Thresholds for thermal damage to normal tissues: an update. International Journal of Hyperthermia. 1;**27**(4):320-43 (2011).
51. Mackey MA, Ali MR, Austin LA, Near RD, El-Sayed MA. The most effective gold nanorod size for plasmonic photothermal therapy: theory and in vitro experiments. The Journal of Physical Chemistry B. 23;**118**(5):1319-26 (2014).
52. Saccomandi P, Schena E, Silvestri S. Techniques for temperature monitoring during laser-induced thermotherapy: An overview. International Journal of Hyperthermia. 1;**29**(7):609-19 (2013).
53. Paulides MM, Stauffer PR, Neufeld E, Maccarini PF, Kyriakou A, Canters RA, Diederich CJ, Bakker JF, Van Rhoon GC. Simulation techniques in hyperthermia treatment planning. International Journal of Hyperthermia. 1;**29**(4):346-57 (2013).